

## Removal of Phenol Using Sulphate Radicals Activated by Natural Zeolite Supported Cobalt Catalysts

Syaifullah Muhammad<sup>1,2</sup>, Edy Saputra<sup>1,3</sup>, Hongqi Sun<sup>1</sup>, H. M. Ang<sup>1</sup>, Moses O. Tadé<sup>1</sup>, Shaobin Wang<sup>1\*</sup>

<sup>1</sup>Department of Chemical Engineering and Cooperative Research Centre for Contamination Assessment and Remediation of the Environment (CRC-CARE), Curtin University, GPO Box U1987, Perth, WA 6845, Australia

<sup>2</sup>Department of Chemical Engineering, Syiah Kuala University, Banda Aceh, Indonesia

<sup>3</sup>Department of Chemical Engineering, Riau University, Pekanbaru, Indonesia

\*Corresponding Author: [Shaobin.wang@curtin.edu.au](mailto:Shaobin.wang@curtin.edu.au)

### Abstract

Two Co oxide catalysts supported on natural zeolites from Indonesia (INZ) and Australia (ANZ) were prepared and used to activate peroxymonosulphate for degradation of aqueous phenol. The two catalysts were characterized by several techniques such as X-ray diffraction (XRD), scanning electron microscopy (SEM), energy dispersive X-ray spectroscopy (EDS), and N<sub>2</sub> adsorption. It was found that Co/INZ and Co/ANZ are effective in activation of peroxymonosulphate to produce sulphate radicals for phenol degradation. Co/INZ and Co/ANZ could remove phenol up to 100% and 70%, respectively, at the conditions of 25 ppm phenol (500 mL), 0.2 g catalyst, 1 g oxone, and 25 °C. Several parameters such as amount of catalyst loading, phenol concentration, oxidant concentration and temperature were found to be the key factors influencing phenol degradation. A pseudo first order would fit to phenol degradation kinetics and the activation energies on Co/INZ and Co/ANZ were obtained as 52.4 and 61.3 kJ/mol, respectively.

**Key words:** Heterogeneous oxidation; sulphate radical; phenol degradation; natural zeolite; Co oxide

## 48 **1. Introduction**

49

50 Phenolic compounds are important organic pollutants in wastewater, which can be produced in  
51 chemical, petrochemical, and pharmaceutical industries (Ahmaruzzaman, 2008, Busca, et al., 2008).  
52 This type of organic contaminants can not be easily removed in primary and secondary treatment  
53 processes. Therefore, it is essential to adopt a tertiary treatment such as thermal oxidation, chemical  
54 oxidation, wet air oxidation, catalytic oxidation etc, which are generally known as advanced  
55 oxidation processes (AOPs) (Parmeggiani and Cardona, 2012, Wang and Xu, 2012, Shukla, et al.,  
56 2010). In principle, the AOPs will produce harmless compounds to the environment such as CO<sub>2</sub>  
57 and H<sub>2</sub>O. Among the AOPs, heterogeneous catalytic oxidation usually has some advantages such as  
58 operating at room temperature with normal pressure and low energy. Furthermore, heterogeneous  
59 catalysts can be synthesized using cheap materials as supports such as activated carbon, silica,  
60 alumina and zeolites (Saputra, et al., 2012). Among the materials, zeolites are important  
61 heterogeneous catalysts used in industry. Their key properties are size and shape selectivity,  
62 together with the potential for strong acidity. Zeolites also have ion exchangeable sites and highly  
63 hydrothermal stability, making them widely used for many applications in separation, ion exchange  
64 and adsorption. Natural zeolites are much cheaper than synthetic zeolites due to their wide  
65 availability in the world (Wang and Peng, 2010). However, few investigations have been reported  
66 in use of natural zeolites for AOPs (Valdes, et al., 2009).

67 Currently, most of AOPs are based on the generation of very reactive species, such as hydroxyl  
68 radicals (OH•), which will oxidize many pollutants quickly and non selectively (Wang and Xu,  
69 2012, Dhakshinamoorthy, et al., 2012, Wang, 2008). Recently, sulphate radicals have also been  
70 proposed as alternative active oxidants due to their higher oxidation potential (Zhou, et al., 2011,  
71 Ling, et al., 2010). For sulphate radical production, peroxymonosulphate (PMS, HSO<sub>5</sub><sup>-</sup>) reaction  
72 with Co ions has been found to be an effective route (Anipsitakis and Dionysiou, 2003, Anipsitakis  
73 and Dionysiou, 2004).

74 However, the use of Co metal ion as a catalyst to activate PMS for generation of sulphate radicals  
75 raises an issue of toxicity of the cobalt ions in water, because Co is one of heavy metals which can  
76 cause diseases to animals and human beings. Thus, employing Co<sup>2+</sup>/PMS for oxidation of aqueous  
77 pollutants and minimizing the discharge of cobalt in wastewater require development of an efficient  
78 heterogeneous catalytic system by incorporating cobalt ions in a substrate. In addition, it is easy to  
79 recover the used catalysts after simple separation process. In the past years, several types of  
80 heterogeneous cobalt catalyst including cobalt oxides (Anipsitakis, et al., 2005, Chen, et al., 2008),  
81 cobalt composite (Yang, et al., 2009) and supported cobalt catalysts have been investigated (Yang,  
82 et al., 2008, Hu, et al., 2011, Shukla, et al., 2010, Shukla, et al., 2010, Shukla, et al., 2011, Shukla,  
83 et al., 2011, Hardjono, et al., 2011).

84 In the previous investigations, synthetic materials were employed and they are usually expensive.  
85 Moreover, some of the supported catalysts did not show good activity. Natural zeolites are cheaper  
86 porous aluminosilicate materials and have been used for adsorbents and catalyst supports. However,  
87 no work has been reported for natural zeolite supported Co catalysts in PMS activation water  
88 treatment. In this research, we investigate cobalt based catalysts supported on Indonesian natural  
89 zeolite (INZ) and Australian natural zeolite (ANZ) for heterogeneous generation of sulphate  
90 radicals for chemical mineralization of phenol in the solution. Several key parameters in the kinetic  
91 study such as phenol concentration, catalyst loading, oxone concentration and temperature were  
92 investigated.

93

94

## 95 **2. Materials and Methods**

96

### 97 **2.1 Synthesis of natural zeolite supported cobalt catalysts**

98

99 Cobalt/Indonesian-natural-zeolite (Co/INZ) and cobalt/Australian-natural-zeolite (Co/ANZ) were  
100 synthesized using an impregnation method. INZ and ANZ samples were crushed in particle size of  
101 60-100  $\mu\text{m}$ . Cobalt nitrate ( $\text{Co}(\text{NO}_3)_2 \cdot 6\text{H}_2\text{O}$ , Sigma-Aldrich) was dissolved into 200 mL ultrapure  
102 water. Then, INZ or ANZ was added into the solution and kept stirring for 24 h. The solid was dried  
103 in an oven at 120  $^\circ\text{C}$  for 6 h. Calcination of the catalysts was conducted in a furnace at 550  $^\circ\text{C}$  for 6  
104 h. For the two catalysts, Co loading was kept at 5 wt%.

### 105 **2.2 Characterization of catalysts**

106

107 The synthesized catalysts were characterized by XRD, SEM combined with EDS, and  $\text{N}_2$   
108 adsorption. Crystalline structure of the materials was analyzed by a X-ray diffractometer (Bruker  
109 D8 Advance equipped with a Lynx eye detector, Bruker-AXS, Karlsruhe, Germany) operated at 40  
110 kV and 30 mA. SEM (Philips XL30) with secondary and backscatter electron detectors at 15 kV  
111 and 7 mm distance was used to obtain a visual image of the samples to show the texture and  
112 morphology of the catalysts with magnification up to 8000 times. The catalysts were also  
113 characterized by EDS (Energy Dispersive X-ray spectroscopy) to identify the structural features and  
114 the mineralogy. Furthermore, nitrogen adsorption (Micromeritics Gemini 2360) was used to obtain  
115 the BET surface area ( $S_{\text{BET}}$ ). Prior to the analysis, the catalyst samples were degassed under vacuum  
116 at 200  $^\circ\text{C}$  for 12 h.

117

### 118 **2.3 Kinetic study of phenol oxidation**

119

120 Catalytic oxidation of phenol was conducted in 500 mL phenol solutions with concentrations of 25 -  
121 100 ppm. A reactor attached to a stand was dipped into a water bath with a temperature control. The  
122 solution was stirred constantly at 400 rpm to maintain a homogeneous solution. A fixed amount of

123 oxidant of peroxymonosulphate (using oxone, DuPont's triple salt  $2\text{KHSO}_5 \cdot \text{KHSO}_4 \cdot \text{K}_2\text{SO}_4$ ,  
124 Aldrich) was added to the mixture until completely dissolved. Then, a fixed amount of catalysts  
125 (Co/INZ or Co/ANZ) was added into the reactor for running of 3-5 h. At the fixed time interval, 0.5  
126 mL of solution sample was withdrawn and filtered using a HPLC standard filter of 0.45  $\mu\text{m}$  and  
127 mixed with 0.5 mL methanol as a quenching reagent to stop the reaction. Phenol was then analyzed  
128 on a HPLC with a UV detector at wavelength of 270 nm. The column is C18 with mobile phase of  
129 70% acetonitrile and 30% ultrapure water.

130

### 131 **3 Results and Discussion**

132

#### 133 **3.1 Characterization of natural zeolite supported cobalt catalysts**

134

135 XRD patterns of Co/INZ and Co/ANZ are presented in Fig.1.  $\text{Co}_3\text{O}_4$  peaks were identified on both  
136 catalysts, however, the peaks are weaker and broad on Co/INZ. This suggested that dispersion of  
137  $\text{Co}_3\text{O}_4$  crystallites on INZ was higher and thus more active sites ( $\text{Co}_3\text{O}_4$ ) were produced on Co/INZ,  
138 which could enhance reaction rate.  $\text{N}_2$  adsorption showed that the BET surface areas of INZ and  
139 ANZ are 30.5 and 16.0  $\text{m}^2/\text{g}$ , respectively, while the BET surface areas of Co/INZ and Co/ANZ are  
140 17.9 and 8.1  $\text{m}^2/\text{g}$ , respectively. In general, high surface area of a support will result in high  
141 dispersion of active metal on the support.

142

143

[Insert Fig.1]

144

145

146 SEM images and EDS spectra of Co/INZ and Co/ANZ catalysts are shown in Fig. 2 and Fig. 3.  
147 Both secondary electron (SE) and backscattered (BSE) detectors were adopted to observe the  
148 dispersion of active cobalt on the catalyst support. From Fig. 2A and 2B, it can be seen that the BSE  
149 detector produces the brighter image than the SE detector at the same observed area. This brighter  
150 area refers to the presence of cobalt specks on Co/INZ particles. It also implies that cobalt was well  
151 dispersed and coated on the natural zeolite support. The presence of cobalt in the catalyst was also  
152 confirmed by EDS spectra (Fig. 2C).

153

[Insert Figure 2]

154

155 A similar observation was also obtained on Co/ANZ catalyst (Fig. 3). However, the particle size of  
156 Co/ANZ seems to be larger than Co/INZ. BSE image also shows a good dispersion of cobalt on  
157 Co/ANZ surface confirmed by EDS spectra. Thus, compared with Co/INZ, Co/ANZ presents larger  
158 particle size but low Co dispersion.

159

160

[Insert Figure 3]

161

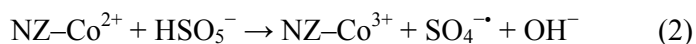
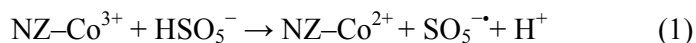
162  
163  
164  
165  
166  
167  
168  
169  
170  
171  
172  
173  
174  
175  
176  
177  
178  
179  
180  
181  
182  
183  
184  
185  
186  
187  
188  
189  
190  
191  
192  
193  
194  
195  
196  
197  
198  
199  
200

### 3.2 Phenol oxidation

Adsorption and oxidation of phenol on Co/INZ and Co/ANZ are presented in Fig. 4. In the presence of only oxone in phenol solution, no phenol degradation occurred, indicating that oxone itself could not produce sulphate radicals to induce phenol oxidation. Both Co/INZ and Co/ANZ presented low adsorption of phenol at less than 10% in 5 h. However, Co/INZ presented a slight higher phenol adsorption than Co/ANZ, which can be ascribed to higher surface area of Co/INZ.

#### [Insert Figure 4]

In oxidation tests, Co/INZ with the presence of PMS could degrade phenol up to 100% in 5 h. Meanwhile, Co/ANZ could reach around 70% phenol removal. Significant degradation of phenol in the systems confirms that cobalt in both catalysts could activate PMS to generate sulphate radicals ( $\text{SO}_4^{\cdot-}$  and  $\text{SO}_5^{\cdot-}$ ) for phenol decomposition in solution. XRD analyses showed that  $\text{Co}_3\text{O}_4$  is major Co species in both catalysts, which will play the role for oxone activation. The reaction mechanism can be listed as below.



Adsorption tests showed that Co/INZ presented higher phenol adsorption than Co/ANZ. XRD also indicated that Co dispersion on Co/INZ is higher than that on Co/ANZ. SEM images show smaller particle size of the catalyst, Co/INZ. For heterogeneous oxidation, high surface adsorption of phenol and more active Co oxide on surface will promote catalytic activity. Thus, Co/INZ exhibits higher activity than Co/ANZ, achieving 100% phenol removal in less time. Some investigations using different supported Co catalysts have been reported. It was reported that Co/ZSM5 could achieve complete degradation of phenol in 6 h (Shukla, et al., 2010) and that Co/SiO<sub>2</sub> could make 100% phenol degradation at 350 min (Shukla, et al., 2011). Therefore, Co/INZ is better than Co/ZSM5 and Co/SiO<sub>2</sub>.

Several variables influencing phenol degradations were also investigated. The effect of initial phenol concentration at 25, 50, 75 and 100 mg/L on phenol degradation is shown in Fig. 5. Phenol degradation efficiency decreased with increasing phenol concentration. The 100% phenol removal could be achieved at phenol concentration of 25 mg/L in 5 h by using Co/INZ catalyst. While in the same duration at phenol concentrations of 50, 75 and 100 mg/L, removal efficiency obtained are 50, 40 and 30%, respectively. For phenol degradation in Co/INZ-oxone, phenol degradation rate is dependent on the concentration of sulphate radicals. Due to the same concentrations of Co/INZ and

201 PMS, sulphate radical concentration produced in solution will be the same. Thus, high amount of  
202 phenol in solution will require more time to achieve the same removal rate, thus lowering phenol  
203 degradation efficiency.

204 **[Insert Figure 5]**  
205

206 Phenol removal efficiency is also affected by catalyst loading in the system as shown in Fig. 6. A  
207 complete removal of phenol could be reached within 5 h at 0.4 g/L Co/INZ loading. While 70% and  
208 40% removals could be reached at Co/INZ loading of 0.2 and 0.1 g/L, respectively. For phenol  
209 degradation, increased catalyst loading would enhance phenol adsorption and Co oxide to activate  
210 PMS, resulting in high phenol degradation.

211 **[Insert Figure 6]**  
212

213 The effect of oxone concentration on the removal efficiency of phenol is presented in Fig. 7. For  
214 both catalysts, higher oxone concentration resulted in higher phenol removal. At reaction time of 3  
215 h, the highest removal efficiency of phenol was obtained at 2 g/L oxone and the lowest was at 0.5  
216 g/L oxone on Co/ANZ. However, phenol degradation would reach a similar level after oxone  
217 loading higher than 1 g/L on Co/INZ, suggesting the optimal loading at 1 g/L.  
218

219 **[Insert Figure 7]**  
220

221 In addition, temperature is also a key factor influencing catalyst activity and phenol degradation.  
222 Fig.8 shows the effect of temperature on phenol degradation. Higher phenol removal was obtained  
223 at increased temperature. For instance, at reaction time of 3 h, removal efficiencies of phenol on  
224 Co/ANZ at 25, 35, and 45 °C were 45, 75 and 100%, respectively (Fig. 8B). A similar trend is also  
225 obtained on Co/INZ catalyst and the removal efficiencies increased from 80% at 25 °C to 100% at  
226 35 and 45 °C.  
227

228 **[Insert Figure 8]**  
229

230 For variation of phenol degradation with time, a first order model as shown in equation below was  
231 used to fit kinetics.  
232

233  
234  
235 
$$C = C_0 e^{(-k \cdot t)} \quad (3)$$

236 Where  $k$  is the first order rate constant of phenol removal,  $C$  is the concentration of phenol at  
237 various time ( $t$ ),  $C_o$  is the initial concentration of phenol.

238 Fig.8 also shows the curves of phenol degradation kinetics from the first order model and it is seen  
239 that phenol degradation on Co/INZ and Co/ANZ catalysts could be well fitted by the model. The  
240 rate constant and regression coefficients are presented in Table 1. Several heterogeneous Co  
241 catalysts have been tested in PMS activation for phenol degradation. It was found that phenol  
242 degradation on Co/SiO<sub>2</sub> (Shukla, et al., 2011) and Co/ZSM5 (Shukla, et al., 2010) presented zero  
243 order kinetics while Co/AC showed the first order kinetics (Shukla, et al., 2010). Chen et al. (Chen,  
244 et al., 2007) also found the pseudo first-order for decolourization of acid orange 7 (AO7) in aqueous  
245 Co<sup>2+</sup>/oxone system.

246

247

**[Insert Table 1]**

248

249 Fig.9 shows the relationship between rate constants ( $k$ ) and temperatures by the Arrhenius  
250 correlation. It can be seen that a good relationship for both catalysts was achieved and activation  
251 energies for phenol degradation on Co/ANZ and Co/INZ were obtained at 52.4 and 61.3 kJ/mol,  
252 respectively.

253

**[Insert Figure 9]**

254

255

#### 256 **4 Conclusions**

257

258 Co/INZ and Co/ANZ are effective catalysts for generating sulphate radicals in the presence of PMS  
259 to degrade phenol. Co/INZ has better activity in removing phenol than Co/ANZ. Phenol removal is  
260 a combination of oxidation and adsorption processes. The concentration of phenol, catalyst loading,  
261 concentration of oxone, and temperature are key parameters affecting the reaction rate in phenol  
262 degradation. Kinetic studies show that phenol oxidation on the Co/INZ and Co/ANZ follows the  
263 first order reaction with the activation energies of 52.4 and 61.3 kJ/mol, respectively.

264

#### 265 **Acknowledgements**

266

267 We thank DIKTI sponsor, National Education Department of Indonesia Government, for providing  
268 a scholarship to SM and ES for their Ph.D study.

269

270

#### 271 **References**

272

273 Ahmaruzzaman, M. (2008). Adsorption of phenolic compounds on low-cost adsorbents: A review,  
274 *Advances in Colloid and Interface Science*, 143, 48-67.

- 275 Anipsitakis, G.P., Dionysiou, D.D. (2003). Degradation of organic contaminants in water with  
276 sulfate radicals generated by the conjunction of peroxymonosulfate with cobalt, *Environ Sci*  
277 *Technol*, 37, 4790-4797.
- 278 Anipsitakis, G.P., Dionysiou, D.D. (2004). Radical generation by the interaction of transition metals  
279 with common oxidants, *Environ Sci Technol*, 38, 3705-3712.
- 280 Anipsitakis, G.P., Stathatos, E., Dionysiou, D.D. (2005). Heterogeneous activation of oxone using  
281  $\text{Co}_3\text{O}_4$ , *J Phys Chem B*, 109, 13052-13055.
- 282 Busca, G., Berardinelli, S., Resini, C., Arrighi, L. (2008). Technologies for the removal of phenol  
283 from fluid streams: A short review of recent developments, *J Hazard Mater*, 160, 265-288.
- 284 Chen, X.Y., Chen, J.W., Qiao, X.L., Wang, D.G., Cai, X.Y. (2008). Performance of nano-  
285  $\text{Co}_3\text{O}_4$ /peroxymonosulfate system: Kinetics and mechanism study using Acid Orange 7 as a  
286 model compound, *Appl Catal B-Environ*, 80, 116-121.
- 287 Chen, X., Qiao, X., Wang, D., Lin, J., Chen, J. (2007). Kinetics of oxidative decolorization and  
288 mineralization of Acid Orange 7 by dark and photoassisted  $\text{Co}^{2+}$ -catalyzed peroxymono  
289 sulfate system, *Chemosphere*, 67, 802-808.
- 290 Dhakshinamoorthy, A., Navalon, S., Alvaro, M., Garcia, H. (2012). Metal Nanoparticles as  
291 Heterogeneous Fenton Catalysts, *Chemosuschem*, 5, 46-64.
- 292 Hardjono, Y., Sun, H.Q., Tian, H.Y., Buckley, C.E., Wang, S.B. (2011). Synthesis of Co oxide  
293 doped carbon aerogel catalyst and catalytic performance in heterogeneous oxidation of phenol  
294 in water, *Chem Eng J*, 174, 376-382.
- 295 Hu, L., Yang, X., Dang, S. (2011). An easily recyclable Co/SBA-15 catalyst: Heterogeneous  
296 activation of peroxymonosulfate for the degradation of phenol in water, *Appl Catal B-*  
297 *Environ*, 102, 19-26.
- 298 Ling, S.K., Wang, S.B., Peng, Y.L. (2010). Oxidative degradation of dyes in water using  $\text{Co}^{2+}/\text{H}_2\text{O}_2$   
299 and  $\text{Co}^{2+}$ /peroxymonosulfate, *J Hazard Mater*, 178, 385-389.
- 300 Parmeggiani, C., Cardona, F. (2012). Transition metal based catalysts in the aerobic oxidation of  
301 alcohols, *Green Chemistry*, 14, 547-564.
- 302 Saputra, E., Muhammad, S., Sun, H., Ang, H.M., Tade, M.O., Wang, S. (2012). Red mud and fly  
303 ash supported Co catalysts for phenol oxidation, *Catal Today*, DOI:  
304 10.1016/j.cattod.2011.10.025.
- 305 Shukla, P., Fatimah, I., Wang, S.B., Ang, H.M., Tade, M.O. (2010). Photocatalytic generation of  
306 sulphate and hydroxyl radicals using zinc oxide under low-power UV to oxidise phenolic  
307 contaminants in wastewater, *Catal Today*, 157, 410-414.
- 308 Shukla, P., Sun, H.Q., Wang, S.B., Ang, H.M., Tade, M.O. (2011). Co-SBA-15 for heterogeneous  
309 oxidation of phenol with sulfate radical for wastewater treatment, *Catal Today*, 175, 380-385.
- 310 Shukla, P., Sun, H.Q., Wang, S.B., Ang, H.M., Tade, M.O. (2011). Nanosized  $\text{Co}_3\text{O}_4/\text{SiO}_2$  for  
311 heterogeneous oxidation of phenolic contaminants in waste water, *Sep Purif Technol*, 77, 230-  
312 236.
- 313 Shukla, P., Wang, S.B., Singh, K., Ang, H.M., Tade, M.O. (2010). Cobalt exchanged zeolites for  
314 heterogeneous catalytic oxidation of phenol in the presence of peroxymonosulphate, *Appl*  
315 *Catal B-Environ*, 99, 163-169.
- 316 Shukla, P.R., Wang, S.B., Sun, H.Q., Ang, H.M., Tade, M. (2010). Activated carbon supported  
317 cobalt catalysts for advanced oxidation of organic contaminants in aqueous solution, *Appl*  
318 *Catal B-Environ*, 100, 529-534.
- 319 Valdes, H., Farfan, V.J., Manoli, J.A., Zaror, C.A. (2009). Catalytic ozone aqueous decomposition  
320 promoted by natural zeolite and volcanic sand, *J Hazard Mater*, 165, 915-922.
- 321 Wang, J.L., Xu, L.J. (2012). Advanced Oxidation Processes for Wastewater Treatment: Formation  
322 of Hydroxyl Radical and Application, *Critical Reviews in Environmental Science and*  
323 *Technology*, 42, 251-325.
- 324 Wang, S. (2008). A Comparative study of Fenton and Fenton-like reaction kinetics in  
325 decolourisation of wastewater, *Dyes Pigments*, 76, 714-720.



326 Wang, S.B., Peng, Y.L. (2010). Natural zeolites as effective adsorbents in water and wastewater  
327 treatment, *Chem Eng J*, 156, 11-24.

328 Yang, Q., Choi, H., Chen, Y., Dionysiou, D.D. (2008). Heterogeneous activation of  
329 peroxymonosulfate by supported cobalt catalysts for the degradation of 2,4-dichlorophenol in  
330 water: The effect of support, cobalt precursor, and UV radiation, *Appl Catal B-Environ*, 77,  
331 300-307.

332 Yang, Q., Choi, H., Al-Abed, S.R., Dionysiou, D.D. (2009). Iron-cobalt mixed oxide nanocatalysts:  
333 Heterogeneous peroxymonosulfate activation, cobalt leaching, and ferromagnetic properties  
334 for environmental applications, *Appl Catal B-Environ*, 88, 462-469.

335 Zhou, G.L., Sun, H.Q., Wang, S.B., Ang, H.M., Tade, M.O. (2011). Titanate supported cobalt  
336 catalysts for photochemical oxidation of phenol under visible light irradiations, *Sep Purif  
337 Technol*, 80, 626-634.

338

339 **List of Tables**

340

341 Table 1 Rate constants at different temperatures for Co/INZ and CCo/ANZ.

342

343

344

345

346

347

348

349

Table 1 Rate constants at different temperatures for Co/INZ and CCo/ANZ.

Catalyst	Temperature (°C)	Rate constant (min <sup>-1</sup> )	R <sup>2</sup>
Co/INZ	25	7.08 x10 <sup>-3</sup>	0.972
	35	0.0116	0.952
	45	0.0269	0.989
Co/ANZ	25	3.19 x10 <sup>-3</sup>	0.991
	35	6.42 x10 <sup>-3</sup>	0.963
	45	0.0151	0.985

350

351

352

353

354

355

356

357

358

359

360

361

362

363

364

365

366

367

368

369

370

371

372

373

374

375

376

377

378

379  
380  
381  
382  
383  
384  
385  
386  
387  
388  
389  
390  
391  
392  
393  
394  
395  
396  
397  
398  
399  
400  
401  
402  
403  
404  
405  
406  
407  
408  
409  
410  
411  
412  
413  
414  
415  
416  
417  
418  
419  
420  
421  
422  
423  
424  
425  
426  
427  
428  
429  
430

## List of Figures

Figure 1 XRD patterns of Co/ANZ and Co/INZ.

Figure 2. SEM images and EDS spectra of Co/INZ, (A) SE Detector, (B) BSE Detector, (C) EDS spectrum.

Figure 3. SEM images and EDS spectra of Co/ANZ, (A) SE Detector, (B) BSE Detector, (C) EDS spectrum.

Figure 4. Phenol reduction with time in adsorption and catalytic oxidation. Reaction condition: 0.4 g/L catalyst, 2 g/L oxone, 25 ppm phenol, 25°C and stirring speed of 400 rpm.

Figure 5. Effect of phenol concentration on phenol degradation using Co/INZ catalyst. Reaction condition: 0.4 g/L catalyst, 2 g/L oxone, 25°C and stirring speed of 400 rpm.

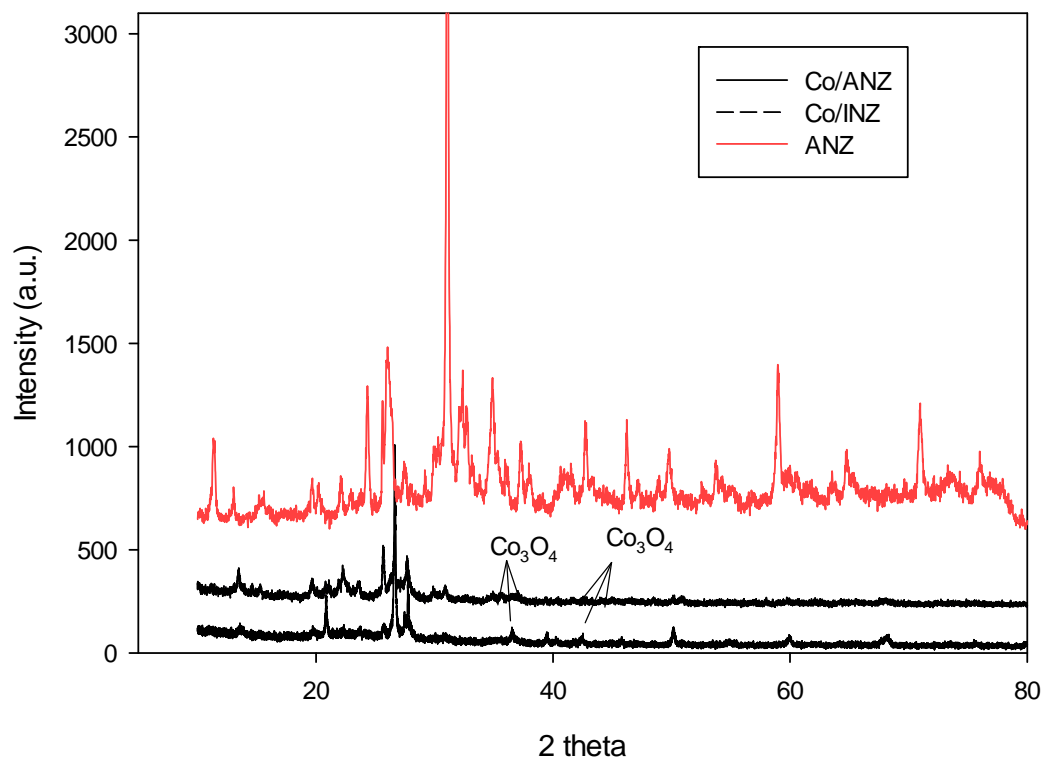
Figure 6. Effect of catalyst loading on phenol degradation using Co/INZ catalyst. Reaction condition: 2 g/L oxone, 25 ppm phenol, 25°C and stirring speed of 400 rpm.

Figure 7. Effect of oxone concentration in phenol reduction using Co/INZ catalyst. Reaction condition : 0.4 g/L catalyst, 25 ppm phenol solution, 25°C and stirring speed of 400 rpm.

Figure 8. Effect of temperature in phenol reduction, (A) Co/INZ catalyst, (B) Co/ANZ catalyst. Reaction condition : 0.4 g/L catalyst, 2 g/L oxone, 25 ppm phenol, and stirring speed of 400 rpm.

Figure 9. Arrhenius plots of phenol degradation on Co/ANZ and Co/INZ.

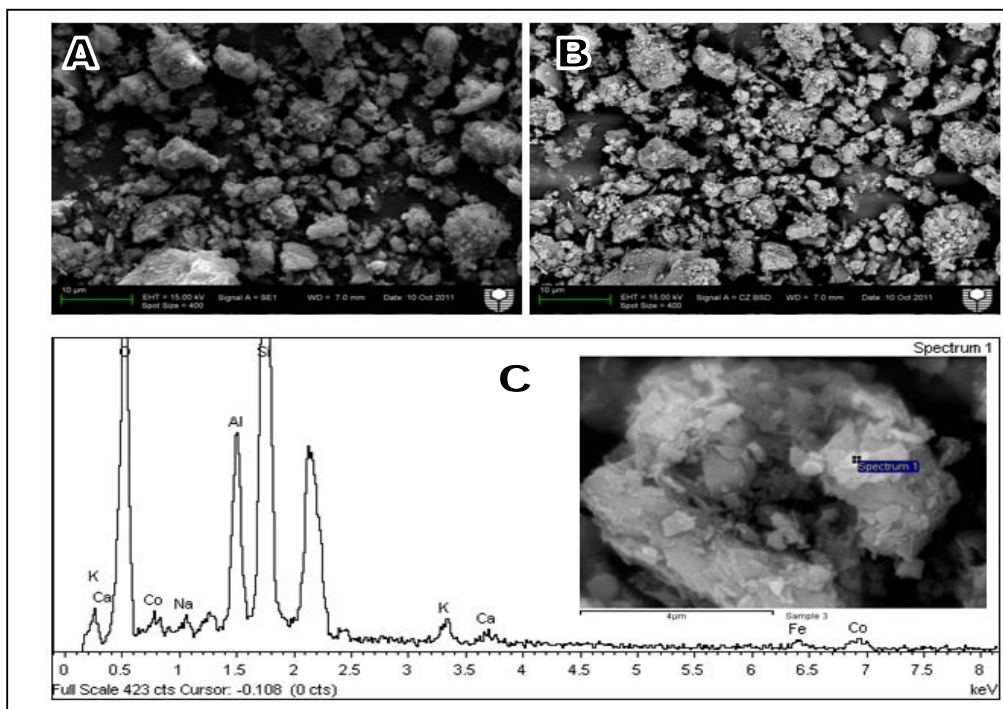
431  
432  
433  
434  
435  
436



437  
438  
439  
440  
441  
442  
443  
444  
445  
446  
447  
448  
449  
450  
451  
452  
453  
454  
455  
456  
457

Fig.1 XRD patterns of Co/ANZ and Co/INZ.

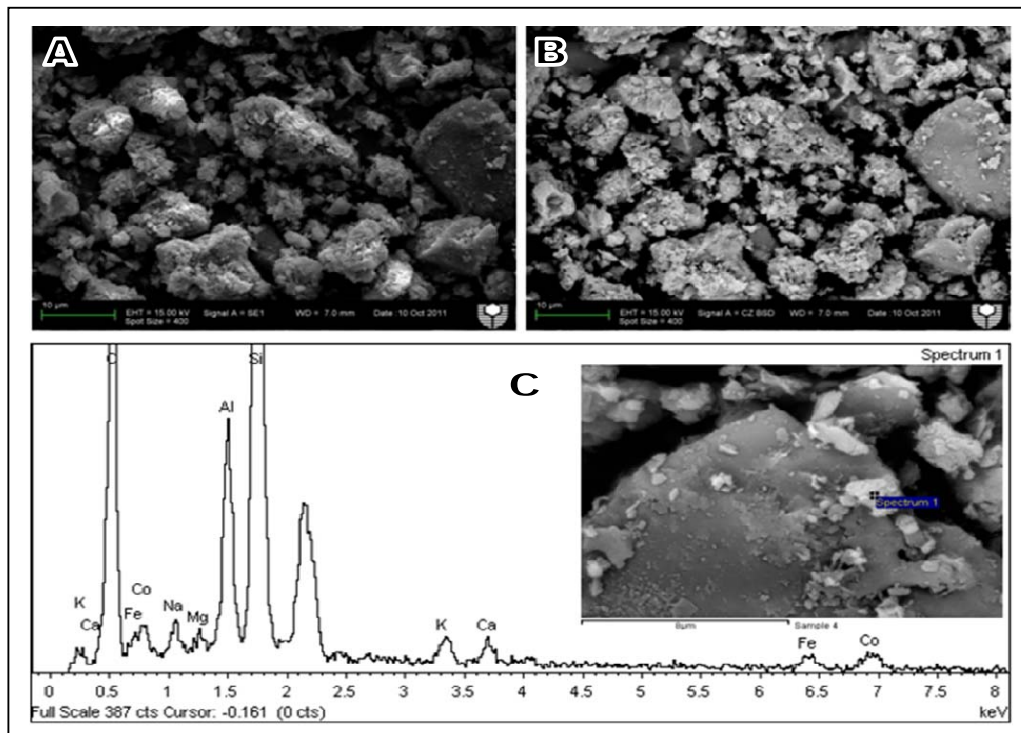
458  
459  
460  
461  
462  
463  
464  
465  
466  
467  
468



469  
470  
471  
472  
473  
474  
475  
476  
477  
478  
479  
480  
481  
482  
483  
484  
485  
486  
487  
488  
489  
490

Figure 2. SEM images and EDS spectra of Co/INZ, (A) SE Detector, (B) BSE Detector, (C) EDS spectra with inset of spectrum image source

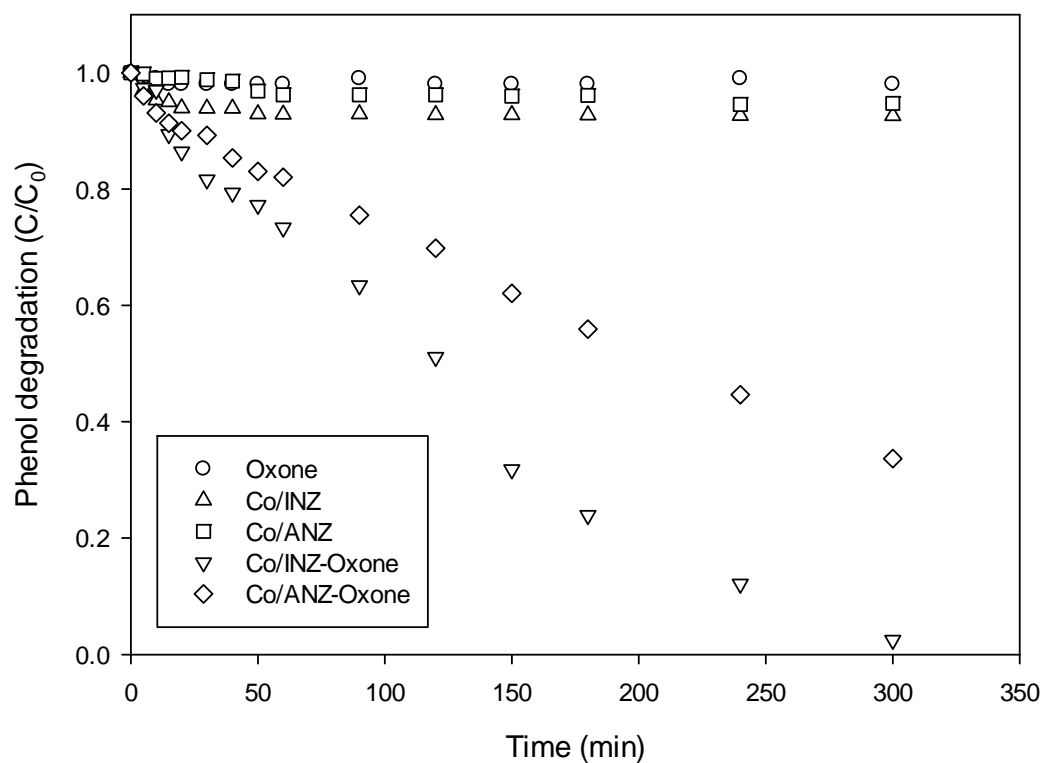
491  
492  
493  
494  
495  
496  
497  
498  
499  
500  
501



502  
503  
504  
505  
506  
507  
508  
509  
510  
511  
512  
513  
514  
515  
516  
517  
518  
519  
520  
521  
522

Figure 3. SEM images and EDS spectra of Co/ANZ, (A) SE Detector, (B) BSE Detector, (C) EDS spectra with inset of spectrum image source

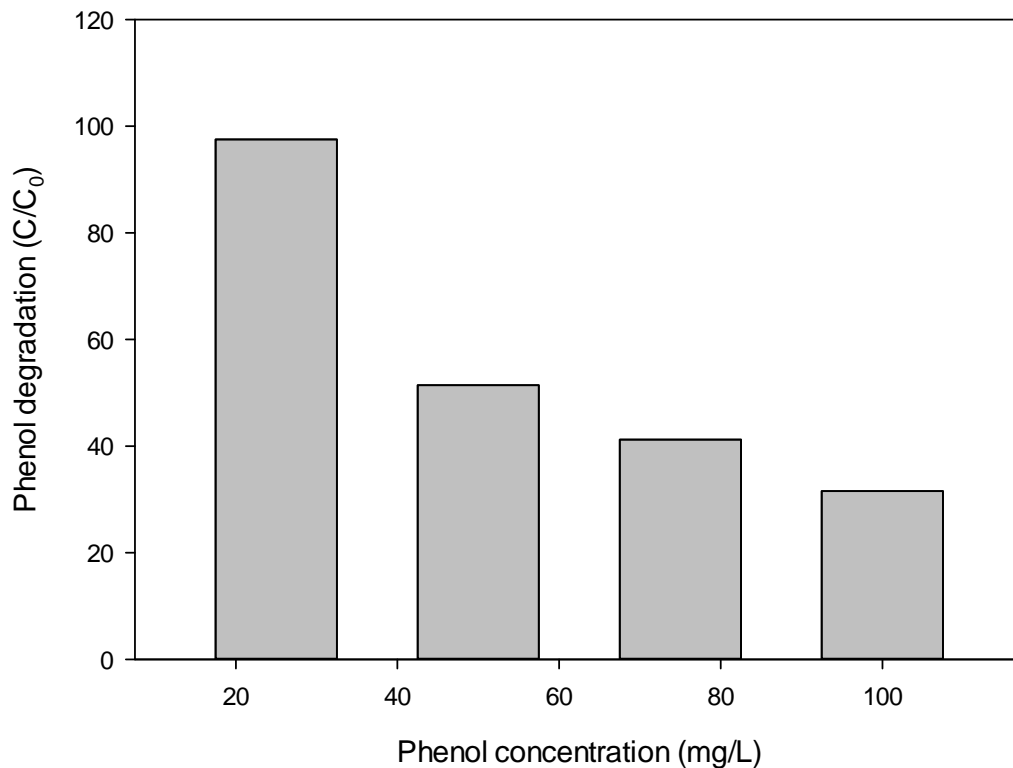
523  
524  
525  
526  
527  
528  
529  
530  
531  
532  
533



534  
535  
536  
537  
538  
539  
540  
541  
542  
543  
544  
545  
546  
547  
548  
549

Figure 4. Phenol reduction with time in adsorption and catalytic oxidation. Reaction condition: 0.4 g/L catalyst, 2 g/L oxone, 25 ppm phenol, 25°C and stirring speed of 400 rpm.

550  
551  
552  
553

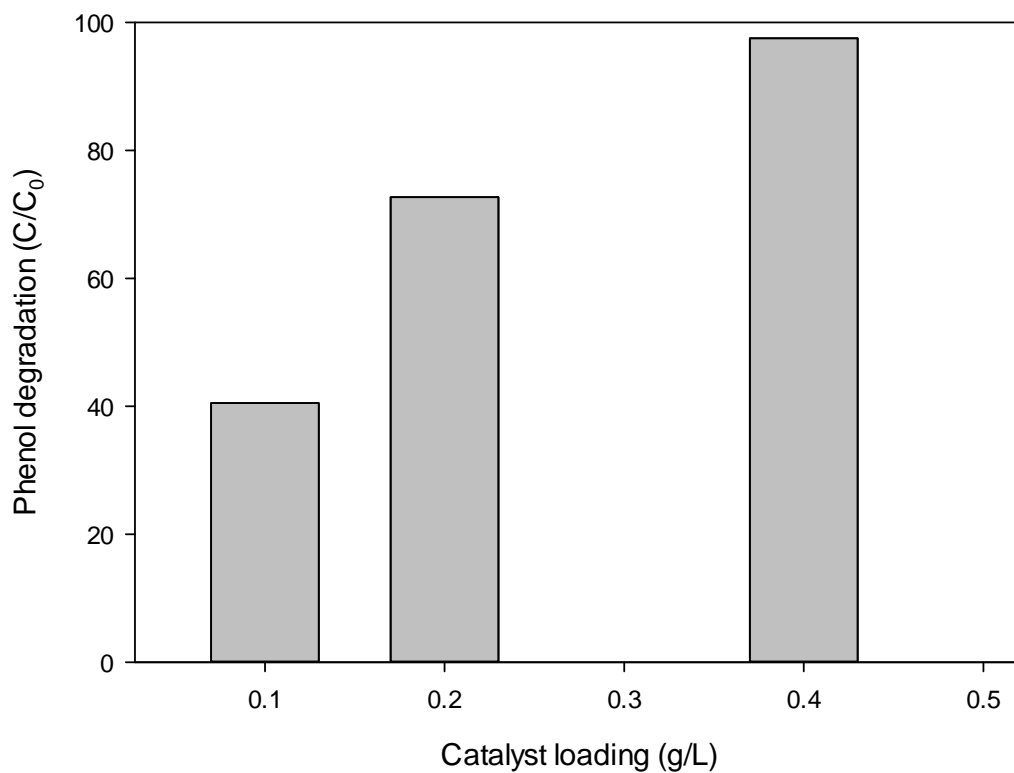


554  
555  
556  
557  
558  
559  
560  
561  
562  
563  
564  
565  
566  
567  
568  
569  
570  
571  
572  
573  
574  
575  
576  
577

Figure 5. Effect of phenol concentration on phenol degradation using Co/INZ catalyst. Reaction condition: 0.4 g/L catalyst, 2 g/L oxone, 25°C and stirring speed of 400 rpm.



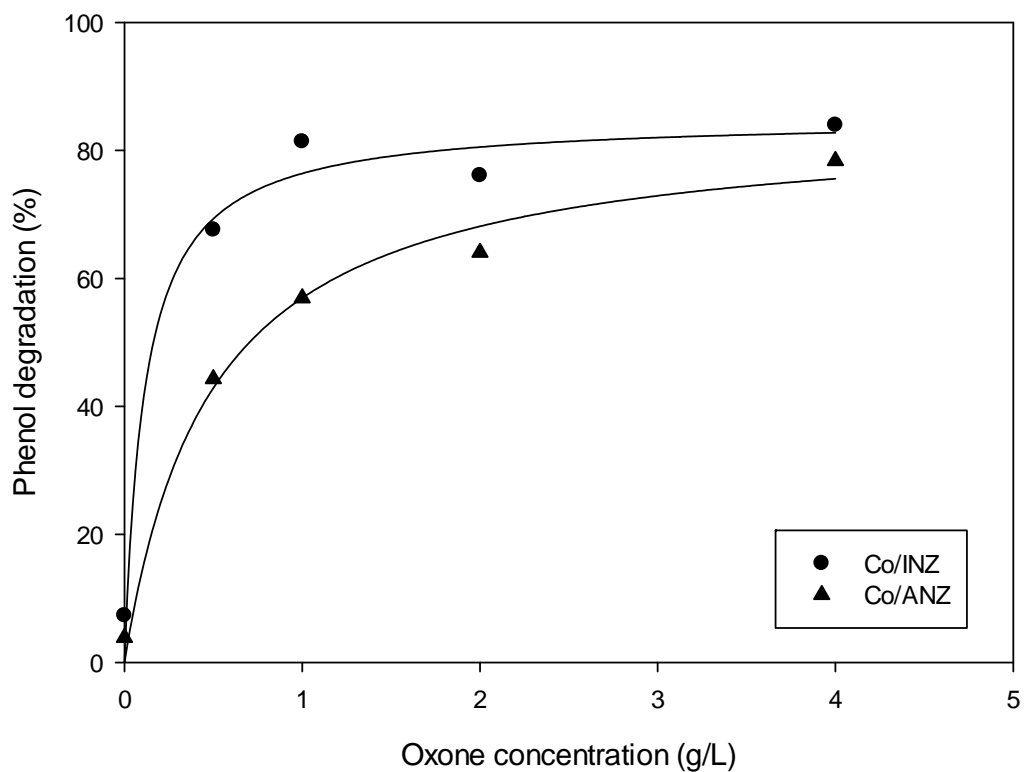
578  
579  
580  
581  
582  
583  
584



585  
586  
587  
588  
589  
590  
591  
592  
593  
594  
595  
596  
597  
598  
599  
600  
601  
602  
603  
604  
605

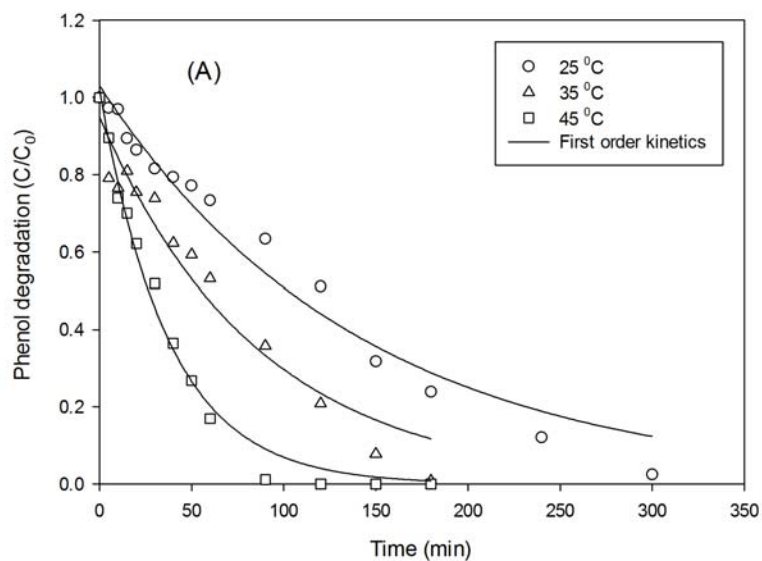
Figure 6. Effect of catalyst loading on phenol degradation using Co/INZ catalyst. Reaction condition: 2 g/L oxone, 25 ppm phenol, 25°C and stirring speed of 400 rpm.

606  
607  
608  
609  
610  
611

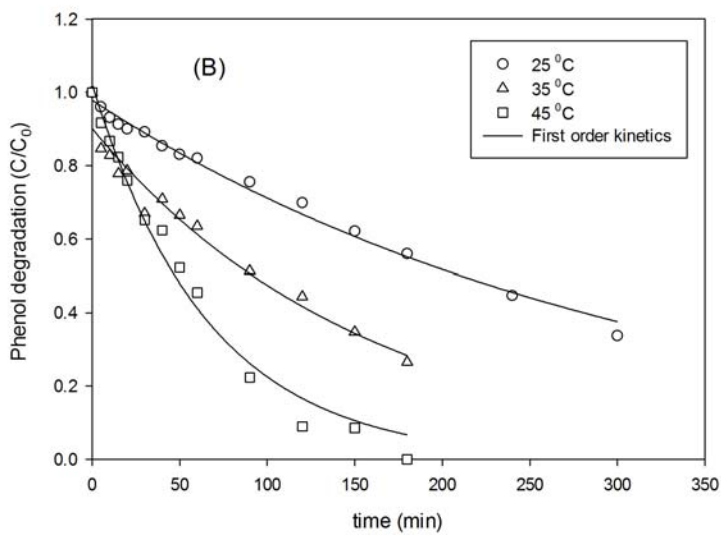


612  
613  
614  
615  
616  
617  
618  
619  
620

Figure 7. Effect of oxone concentration in phenol reduction using Co/INZ catalyst. Reaction condition : 0.4 g/L catalyst, 25 ppm phenol solution, 25°C and stirring speed of 400 rpm.



621



622

623 Figure 8. Effect of temperature in phenol reduction, (A) Co/INZ catalyst, (B) Co/ANZ catalyst.

624 Reaction condition : 0.4 g/L catalyst, 2 g/L oxone, 25 ppm phenol, and stirring speed of 400 rpm.

625

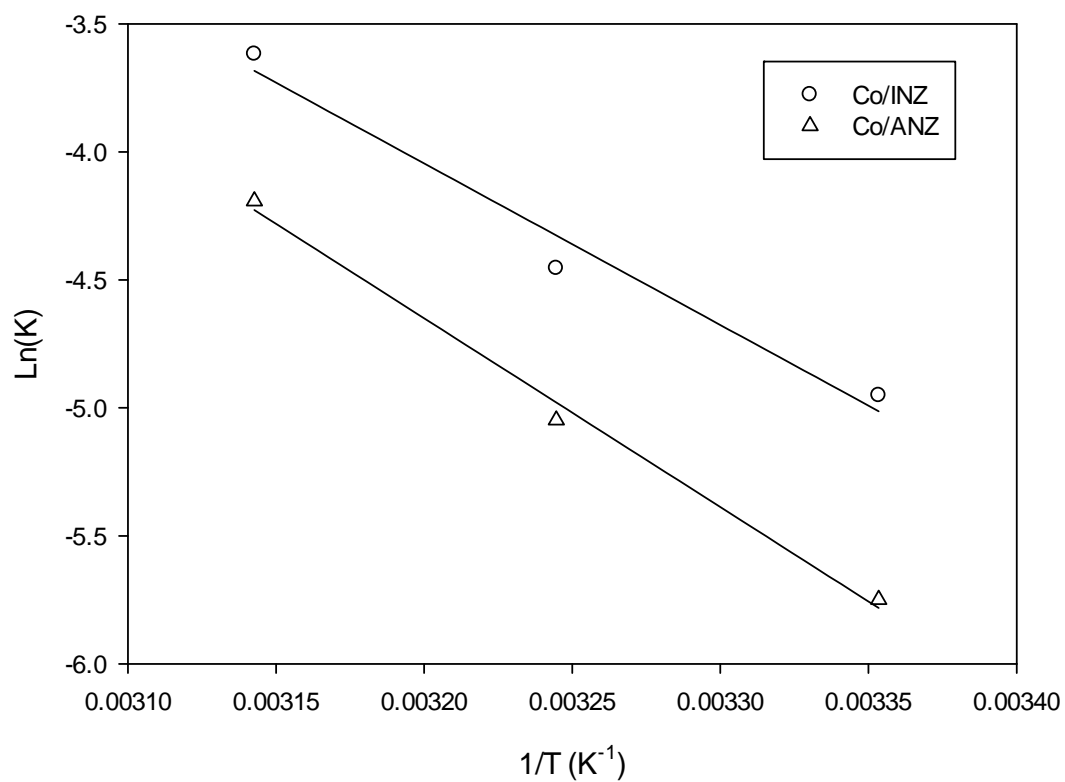
626

627

628

629

630  
631  
632  
633  
634  
635  
636  
637  
638  
639



640  
641  
642  
643  
644  
645

Figure 9. Arrhenius plots of phenol degradation on Co/ANZ and Co/INZ.